IHEP 94-10

V.V. Kiselev, A.K. Likhoded, M.V. Shevlyagin[1]

FOUR HEAVY QUARK AND BOUND STATE PRODUCTION IN THE $e^+e^- \to Q + \bar{Q}' + Q' + \bar{Q}$ and $e^+e^- \to (Q\bar{Q}') + Q' + \bar{Q}$ PROCESSES IN Z^0-BOSON POLE

Submitted to *Yad. Phys.*

[1]Moscow Institute of Physics and Technology

ПРЕПРИНТ 94-10, ИФВЭ, 1994

Protvino 1994

UDK 539.1.01

M-24

Abstract

Kiselev V.V. et al. Four Heavy Quark and Bound State Production in the $e^+e^- \to Q + \bar{Q}' + Q' + \bar{Q}$ and $e^+e^- \to (Q\bar{Q}') + Q' + \bar{Q}$ Processes in Z^0-Boson Pole: IHEP Preprint 94-10. Protvino, 1994. – p. 31, figs. 11, tables 4, refs.: 23.

In the frame of the QCD perturbation theory and nonrelativistic model of heavy quarkonium the cross-sections of four heavy quark production in e^+e^- annihilation, as well as the cross-sections of the associative production of the $1S$- and $2S$-wave $(Q\bar{Q}')$-mesons in the $e^+e^- \to (Q\bar{Q}') + Q' + \bar{Q}$ process are calculated. Basing on the assumption of the quark-hadron duality the number of the Λ_{bc}-hyperons expected for LEP experiments is estimated. The fragmentation functions of b-quark into $B_c(B_c^*)$-meson, c- and b-quarks into $\eta_c(\psi)$- and $\eta_b(\Upsilon)$-mesons, respectively, are obtained.

Аннотация

Киселев В.В. и др. Рождение четырех тяжелых кварков и связанных состояний в процессах $e^+e^- \to Q + \bar{Q}' + Q' + \bar{Q}$ и $e^+e^- \to (Q\bar{Q}') + Q' + \bar{Q}$ в полюсе Z^o-бозона: Препринт ИФВЭ 94-10. – Протвино, 1994. – 31 с., 11 рис., 4 табл., библиогр.: 23.

В рамках теории возмущений КХД и в нерелятивистской модели тяжелого кваркония вычислены сечения рождения в e^+e^- аннигиляции четырех тяжелых кварков, а также сечения ассоциативного рождения $1S$- и $2S$-волновых состояний $(Q\bar{Q}')$-мезонов в процессе $e^+e^- \to (Q\bar{Q}') + Q' + \bar{Q}$. На основе предположения о кварк-адронной дуальности оценивается ожидаемое на LEP количество Λ_{bc}-гиперонов. Получены функции фрагментации b-кварка в $B_c(B_c^*)$-мезон, а также c- и b-кварков в $\eta_c(\psi)$- и $\eta_b(\Upsilon)$-мезоны, соответственно.

INTRODUCTION

The study of the heavy quark production processes is of great interest since it gives an answer, if QCD can be applied, for the description of the heavy quark production and hadronization mechanisms. Features of 2- and 3-jet events have been investigated in detail at the PETRA, KEK, SLC and LEP colliders. In the view of the expected high luminosity ($\sim 10^7 Z^0$) of the LEP collider it becomes interesting to explore more rare multiquark processes. One of these processes is the four quark ($Q\bar{Q}Q'\bar{Q}'$, where $Q(Q')$ is b or c-quark) production in e^+e^- annihilation. We will consider this process, first, as a test of QCD in higher orders $O(\alpha_s^2)$ of the perturbation theory and, secondly, as a step forward in understanding the production, for example, of the bound $b\bar{c}$ ($\bar{b}c$) states, which have not yet been discovered.

The b- and $\bar{c}$-quarks (B_c-mesons) bound states occupy an intermediate position between the J/ψ- and Υ meson families in the mass spectrum. In this sense, the predictions of the nonrelativistic quark model well describing the J/ψ- and Υ meson families can also be applied to B_c-mesons. So, the discovery and investigation of B_c mesons could be a good test for QCD and QCD-inspired nonrelativistic potential models.

The B_c meson production processes in e^+e^-, $p\bar{p}$, and neutrino-hadron collisions have been studied in [1-7]. The B_c meson spectroscopy has been analyzed in [8], and different aspects of B_c meson decays have been considered in [9-11]. The method of helicity amplitude calculations suggested in this paper and Monte-Carlo integration over phase space allows one to obtain all interesting distributions over kinematical variables of both B_c meson and associated particles.

Using exact formulas of the QCD perturbation theory we calculate the cross-section $\sigma(e^+e^- \to cc\bar{c}\bar{c})$, $\sigma(e^+e^- \to b\bar{b}c\bar{c})$, $\sigma(e^+e^- \to bb\bar{b}\bar{b})$, as well as the

cross-section of heavy quarkonium production ($Q\bar{Q}'$) ($Q\bar{Q}' = \psi, B_c, \Upsilon$) for the $e^+e^- \to (Q\bar{Q}') + Q' + \bar{Q}$ processes in nonrelativistic approximation for ($Q\bar{Q}'$). We consider these two processes in one paper for they are closely connected with each other. The method of the helicity amplitude calculation for the $e^+e^- \to Q + \bar{Q}' + Q' + \bar{Q}$ process can be used practically in the same form for the calculation of the $e^+e^- \to (Q\bar{Q}') + Q' + \bar{Q}$ cross-section. If one assumes that the approximate quark-hadron duality is valid, then the $e^+e^- \to Q + \bar{Q}' + Q' + \bar{Q}$ cross-section in the region of small invariant masses of the ($Q\bar{Q}'$)-pair can be related to the production cross-section of the ($Q\bar{Q}'$) meson bound states in the $e^+e^- \to (Q\bar{Q}') + Q' + \bar{Q}$ process.

Using the assumption of quark-hadron duality one can also draw definite conclusions on the cross-section of the $\Lambda_{QQ'}$-hyperon production, where this hyperon is a bound system of two heavy and one light valent quarks of different flavours.

The investigation of the heavy quark fragmentation functions is of great interest from both theoretical and experimental points of view, especially, with respect to the possibility to perform experimental measurements in the Z^0-boson pole, where the bulk of the events is related to the b- and c-quark production. From the theoretical point of view, the fragmentation is described by: 1) perturbative evolution equations including the summation over soft gluon contributions [12]; 2) nonperturbative contributions connected with counting the wave function of a meson in the final state. The standard procedure of taking these two factors into account is reduced to the convolution of the perturbative evolution kernel with nonperturbative fragmentation function. As it is known (see, for example, [12]), in the case of heavy Q-quark fragmentation into meson $Q\bar{q}$, composed of heavy (Q) and light (q) quarks, the role of the nonperturbative contribution is rather important. The situation changes drastically when one discusses heavy Q-quark fragmentation into the system, where the second antiquark $\bar{Q}'$ is heavy too, $Q \to (Q\bar{Q}') + Q'$. In this case the typical virtualities in the process are large ($\geq 4m^2_{Q'}$) and the dependence on the particular form of the ($Q\bar{Q}'$)-meson wave function becomes unessential, and the main features of the fragmentation function behaviour are determined by the QCD perturbation theory. Despite the fact that the main method of calculating such process, as it was mentioned above, is the Monte-Carlo method, in this paper we also have obtained analytical expressions for the $b \to B_c(B_c^*)$, $c \to \eta_c(\psi)$, and $b \to \eta_b(\Upsilon)$ fragmentation functions in the scale limit. These expressions are compared with the result of the precise calculations.

The parer is organized as follows. In Section 1 we present the technique of the matrix element calculation in terms of helicity quark states for processes

with four fermions in the final states. In Section 2 we give the numerical values for the $\sigma(e^+e^- \to b\bar{b}c\bar{c})$ process cross-section, and in Section 3 we present analogous calculations for the processes with quarks of the same flavour in the final state. The calculation method, as well as the cross-section values for the processes with pseudoscalar B_c- and vector B_c^*-meson production are given in Section 4. Section 5 is devoted to characteristic features of the meson production processes, where these mesons are composed of quarks of the same flavour. Analytical expressions for the fragmentation functions of a heavy quark are given in Section 6. In this Section we also analyze the relation of the resulting fragmentation function with phenomenological Peterson parameterization. Section 7 contains conclusions.

1. METHOD OF THE CROSS-SECTION CALCULATION FOR FOUR HEAVY QUARK PRODUCTION

First, let us consider the production of quark with different flavours. For the process of two heavy quark ($Q\bar{Q}$ and $Q'\bar{Q}'$) pair production

$$e^+(q_1) + e^-(q_2) \to Q(p_1) + \bar{Q}(p_2) + Q'(p_3) + \bar{Q}'(p_4) \qquad (1)$$

in the Born approximation 8 Feynman diagrams (4 with photon exchange and 4 with Z^0-boson exchange in the s-channel, see Fig.1) will contribute.

The standard calculation methods for these diagrams by squaring the amplitude lead to extremely cumbersome expressions. In literature, however, there are some works devoted to the cross-section calculations for the processes with four heavy quarks in the final state. For example, the authors of [13] have investigated the $gg \to Q\bar{Q}Q'\bar{Q}'$ process for the case of massless quarks in the frame of the perturbative QCD, and the authors of [14] have also studied the case of massive quarks. In paper [15] the cross-section of the four quark production in the e^+e^--annihilation, $e^+e^- \to Q\bar{Q}Q'\bar{Q}'$ has been calculated for the case of massless quarks by means of the spinor products method [16]. In the present work for the analysis of the $e^+e^- \to Q\bar{Q}Q'\bar{Q}'$ process, where it is necessary to take the quark masses into account, we will use a more convenient, from our point of view, calculation method [14], namely, the method of the direct numerical calculation of the amplitude.

For concreteness, in this section we will imply that Q is the b-quark and Q' is the c-quark. Let us introduce the following notations for the quark momenta:

$$q_{12} = q_1 + q_2\,, \qquad p_{12} = -p_1 - p_2\,, \qquad p_{34} = -p_3 - p_4\,,$$
$$p_{124} = p_{12} - p_4\,, \quad p_{123} = -p_{12} + p_3\,, \quad p_{342} = p_{34} - p_2\,, \quad p_{341} = -p_{34} + p_1$$

and for the currents

$$J^\mu_\gamma = Q^e \frac{\bar v(q_2)\gamma^\mu u(q_1)}{q^2_{12}}\,, \tag{2}$$

$$J^\mu_Z = \frac{\bar v(q_2)\gamma^\mu(v^e_Z - a^e_Z\gamma^5)u(q_1)}{q^2_{12} - M^2_Z + iM_Z\Gamma_Z}\,, \tag{3}$$

$$J^\mu_b = \frac{\bar u(p_1)\gamma^\mu v(p_2)}{p^2_{12}}\,, \tag{4}$$

$$J^\mu_c = \frac{\bar u(p_3)\gamma^\mu v(p_4)}{p^2_{34}} \tag{5}$$

as well as the following additional spinors

$$v_{124} = \frac{(\hat p_{124} + m_c)}{p^2_{124} - m^2_c}\hat J_b v(p_4)\,, \tag{6}$$

$$v_{342} = \frac{(\hat p_{342} + m_b)}{p^2_{342} - m^2_b}\hat J_c v(p_2)\,, \tag{7}$$

$$\bar u_{123} = \bar u(p_3)\hat J_b \frac{(\hat p_{123} + m_c)}{p^2_{123} - m^2_c}\,, \tag{8}$$

$$\bar u_{341} = \bar u(p_1)\hat J_c \frac{(\hat p_{341} + m_b)}{p^2_{341} - m^2_b}. \tag{9}$$

In terms of the values introduced above the amplitude of the $e^+e^- \to b\bar b c\bar c$ process has the form $M = \sum_{i=1}^4 M_i$, where

$$M_1 = \bar u_{341}[\hat J_\gamma Q^b + \hat J_Z(v^b_Z - a^b_Z\gamma^5)]v(p_2)\,, \tag{10}$$
$$M_2 = \bar u(p_1)[\hat J_\gamma Q^b + \hat J_Z(v^b_Z - a^b_Z\gamma^5)]v_{342}\,, \tag{11}$$
$$M_3 = \bar u_{123}[\hat J_\gamma Q^c + \hat J_Z(v^c_Z - a^c_Z\gamma^5)]v(p_4)\,, \tag{12}$$
$$M_4 = \bar u(p_3)[\hat J_\gamma Q^c + \hat J_Z(v^c_Z - a^c_Z\gamma^5)]v_{124}\,, \tag{13}$$
$$M = M_1 + M_2 + M_3 + M_4\,. \tag{14}$$

Here Q^e, Q^b, Q^c and v^e_Z, a^e_Z, v^b_Z, a^b_Z, v^c_Z, a^c_Z are the electromagnetic charges, vector and axial couplings to Z^0-boson for electron, b- and c-quarks.

The amplitude squared should be calculated as the sum over $2^6 = 64$ independent fermion states. We choose the eigen values of the helicity operator $(\vec\Sigma\vec p)$ as two independent states of the ψ spinor:

$$(\vec\Sigma\vec p)\psi(p,\lambda) = \lambda\psi(p,\lambda)\,. \tag{15}$$

To determine the spinors with given values of 4-momentum, p and helicity, $\lambda = \pm 1$, one should choose a particular representation. We will use the spinor (Weil) representation:

$$\gamma^0 = \begin{pmatrix} 0 & 1 \\ 1 & 0 \end{pmatrix} \qquad \vec\gamma = \begin{pmatrix} 0 & -\vec\sigma \\ \vec\sigma & 0 \end{pmatrix} \qquad \vec\Sigma = \begin{pmatrix} \vec\sigma & 0 \\ 0 & \vec\sigma \end{pmatrix}, \tag{16}$$

where

$$\vec\sigma = \{\sigma_x, \sigma_y, \sigma_z\} = \left\{\begin{pmatrix} 0 & 1 \\ 1 & 0 \end{pmatrix}, \quad \begin{pmatrix} 0 & -i \\ i & 0 \end{pmatrix}, \quad \begin{pmatrix} 1 & 0 \\ 0 & -1 \end{pmatrix}\right\}. \tag{17}$$

The particle spinors, $u(p,\pm)$, in this representation take the form:

$$u(p,+) = \frac{1}{\sqrt{2|\vec p|(|\vec p| + p_z)}} \begin{pmatrix} \sqrt{E+|\vec p|}\,(|\vec p| + p_z) \\ \sqrt{E+|\vec p|}\,(p_x + ip_y) \\ \sqrt{E-|\vec p|}\,(|\vec p| + p_z) \\ \sqrt{E-|\vec p|}\,(p_x + ip_y) \end{pmatrix}. \tag{18}$$

$$u(p,-) = \frac{1}{\sqrt{2|\vec p|(|\vec p| + p_z)}} \begin{pmatrix} \sqrt{E-|\vec p|}\,(-p_x + ip_y) \\ \sqrt{E-|\vec p|}\,(|\vec p| + p_z) \\ \sqrt{E+|\vec p|}\,(-p_x + ip_y) \\ \sqrt{E+|\vec p|}\,(|\vec p| + p_z) \end{pmatrix}. \tag{19}$$

The antiparticle spinors, $v(p,\pm)$, are defined as follows

$$v(p,\pm) = Cu^*(p,\mp)\,, \tag{20}$$

where $C = i\gamma^2$ is the matrix of charge conjugation.

The explicit form of the $v(p,\pm)$ spinors is

$$v(p,+) = \frac{1}{\sqrt{2|\vec p|(|\vec p| + p_z)}} \begin{pmatrix} -\sqrt{E+|\vec p|}\,(|\vec p| + p_z) \\ -\sqrt{E+|\vec p|}\,(p_x + ip_y) \\ \sqrt{E-|\vec p|}\,(|\vec p| + p_z) \\ \sqrt{E-|\vec p|}\,(p_x + ip_y) \end{pmatrix}. \tag{21}$$

$$v(p,-)=\frac{1}{\sqrt{2|\vec{p}|(|\vec{p}|+p_z)}}\begin{pmatrix}\sqrt{E-|\vec{p}|}\,(-p_x+ip_y)\\ \sqrt{E-|\vec{p}|}\,(|\vec{p}|+p_z)\\ -\sqrt{E+|\vec{p}|}\,(-p_x+ip_y)\\ -\sqrt{E+|\vec{p}|}\,(|\vec{p}|+p_z)\end{pmatrix}. \qquad (22)$$

In the case of $p_z=-|\vec{p}|$

$$u(p,+)=\begin{pmatrix}0\\ \sqrt{E+|p|}\\ 0\\ \sqrt{E-|p|}\end{pmatrix}, \qquad u(p,-)=\begin{pmatrix}-\sqrt{E-|p|}\\ 0\\ -\sqrt{E+|p|}\\ 0\end{pmatrix}. \qquad (23)$$

$$v(p,+)=\begin{pmatrix}0\\ -\sqrt{E+|p|}\\ 0\\ \sqrt{E-|p|}\end{pmatrix}, \qquad v(p,-)=\begin{pmatrix}-\sqrt{E-|p|}\\ 0\\ \sqrt{E+|p|}\\ 0\end{pmatrix}. \qquad (24)$$

The structure of the color coefficients for the $e^+e^-\to b\bar{b}c\bar{c}$ process is very simple. The color factor, F, corresponding to this process is $F=(N^2-1)/4$, where N=3 is the color number.

The above expressions allowing one to calculate the amplitudes for the $e^+e^-\to b\bar{b}c\bar{c}$ process can be easily transferred to the FORTRAN codes. The resulting program performs calculations very fast and has small size.

We have checked that our programs (two independent programs have been written) for calculation of the squared amplitude summed over all helicity states satisfy the test on Lorentz invariance (boost along the beam axis), as well as the test on azimuthal invariance with respect to the substitutions $p_x\to p_y$ and $p_y\to -p_x$ for the particle momentum. The results of our programs coincide within the calculation accuracy.

The integration over the phase space of the final particles was performed by the Monte-Carlo method by means of a specially developed program package, which generates the values of final particle momenta with the minimization of the weight spread.

2. CROSSS-SECTION OF THE $b\bar{b}c\bar{c}$ PRODUCTION IN THE Z^0 BOSON POLE IN THE FRAME OF QCD PERTURBATION THEORY

In our numerical calculation we will choose a standard set of electroweak theory parameters $M_Z=91.17$ GeV, $\sin^2\theta_W=0.23$, $m_b=4.7$ GeV, $m_c=1.4$ GeV. We take the QCD coupling constant, α_s, as

$$\alpha_s(Q^2)=\frac{12\pi}{(33-2n_f)\ln(Q^2/\Lambda^2)},$$

where $\Lambda=100$ MeV, so as at $Q^2=M_Z^2$ and $n_f=5$ we have $\alpha_s(M_Z)=0.12$ in correspondence with [17].

. From the form of the diagrams in Fig.1 it is evident that the main contribution to the cross-section of the $e^+e^-\to b\bar{b}c\bar{c}$ process comes from diagrams $1a,b$, since for these diagrams the virtual gluon approaches closely the on-sheil state due to the smallness of the c quark mass [6].

The $e^+e^-\to b\bar{b}c\bar{c}$ process appears in the second order of QCD coupling constant, $\alpha_s(Q^2)$. So, a very important problem is to choose the characteristic transferred momentum value, Q^2, in the argument of $\alpha_s(Q^2)$. A characteristic scale for the $\alpha_s(Q^2)$ running constant can be determined by the typical gluon virtuality ($M^2_{c\bar{c}}\sim 4m_c^2$), however, the b-quark virtuality can be much larger and be of the order of s [6], so we will present here the results for two different sets, $Q^2=(4m_c^2,s)$. The $e^+e^-\to b\bar{b}c\bar{c}$ process cross-sections for these cases depending on the total energy of the beams, $\sqrt{s}$, are given in Table 1.

As one can see from this Table, the differences in determining α_s result in the difference of the cross-sections by some orders of magnitude. For the most important energy region (near the Z^0-boson pole) this difference reaches the factor of 3.4. Such strong dependence on α_s is connected with the fact that the $e^+e^-\to b\bar{b}c\bar{c}$ process cross-section is proportional to α_s^2. So, the precise experimental determination of the $e^+e^-\to b\bar{b}c\bar{c}$ process cross-section can allow one to make conclusions on the α_s value in these processes.

Let us define the ratio:

$$R_{b\bar{b}c\bar{c}}=\frac{\sigma(e^+e^-\to b\bar{b}c\bar{c})}{\sigma(e^+e^-\to b\bar{b})}.$$

According to our calculations the $R_{b\bar{b}c\bar{c}}$ value is $R_{b\bar{b}c\bar{c}}=0.8\cdot 10^{-2}$ for $Q^2=s$ and $R_{b\bar{b}c\bar{c}}=2.6\cdot 10^{-2}$ for $Q^2=4m_c^2$. These values obtained from the explicit formulas of the QCD perturbation theory are to be compared with the estimate resulting from the Monte-Carlo program HERWIG (version 5.0), $R_{b\bar{b}c\bar{c}}=(0.8\div 1.8)\cdot 10^{-2}$ [18].

Table 1. The $e^+e^-\to b\bar{b}c\bar{c}$ process cross-section dependence on the total energy of the beams, $\sqrt{s}$, for $\alpha_s(Q^2=4m_c^2)=0.22$ and $\alpha_s(Q^2=s)$. In the brackets we point out the uncertainty (one standard deviation) in the last figure, which is due to the Monte-Carlo method.

$\sqrt{s}$, GeV	30	50	70	91.17	200	500
$\sigma(4m_c^2)$, pb	0.1294(9)	0.217(3)	0.593(9)	234.2(7)	0.254(8)	0.073(5)
$\sigma(s)$, pb	0.0552(4)	0.0782(9)	0.192(3)	69.7(2)	0.061(2)	0.014(1)

3. CROSS-SECTIONS OF THE $c\bar{c}c\bar{c}$ AND $b\bar{b}b\bar{b}$ PRODUCTION IN THE Z^0 BOSON POLE

To calculate the cross-section of the $QQ\bar{Q}\bar{Q}$ system production with the same quarks one ought to take into account the same diagrams as in Fig.1 (with substitution $Q' \to Q$), as well as to take into account the identity of the quarks in the final state. This means that it is necessary to double the number of the diagrams in Fig.1. Thus, the total amplitude can be represented in the following form: $M_{tot} = C_1 \Sigma_{i=1}^4 M_i - C_2 \Sigma_{i=1}^4 \bar{M}_i$, where C_1 and C_2 are the color factors. As for the $\bar{M}_i$ amplitudes, they can easily be obtained in terms of M_i: $\bar{M}_i(p_1,p_2,p_3,p_4) = M_i(p_1,p_4,p_3,p_2)$, i.e. one should permutate the 4-momenta of the identical particles, for example, $p_2 \to p_4$ and $p_4 \to p_2$. As a result of the trace calculation over color degrees of freedom we get $C_1C_1^+ = C_2C_2^+ = (N^2-1)/4$ and $C_1C_2^+ = C_1C_2^+ = -(N^2-1)/(4N)$.

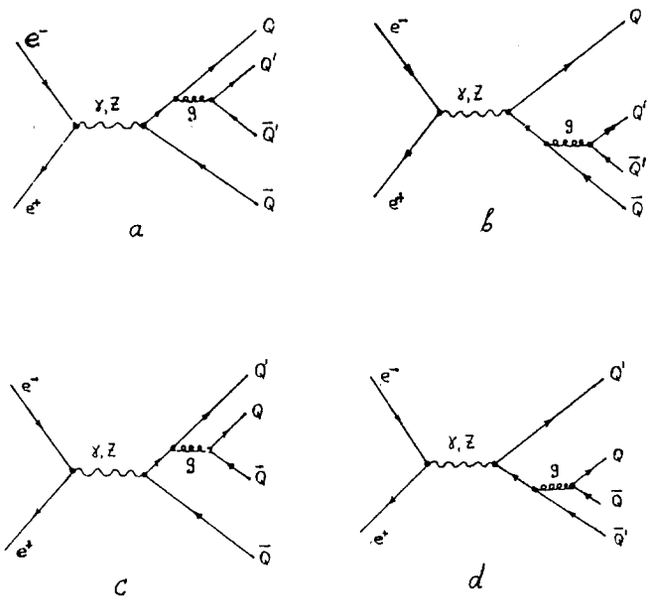

Fig. 1. Feynman diagrams for the $e^+e^- \to Q + \bar{Q}' + Q' + \bar{Q}$ process.

The cross-section calculations for the four c- and b-quarks production according to the scheme described in Section 1 give the following values: $\sigma(e^+e^- \to c\bar{c}c\bar{c})$=168(1) pb (for $\alpha_s(Q^2 = 4m_c^2)$=0.22), $\sigma(e^+e^- \to c\bar{c}c\bar{c})$=50.1(3) pb (for $\alpha_s(Q^2 = M_Z^2)$=0.12), and $\sigma(e^+e^- \to b\bar{b}b\bar{b})$=21.26(5) pb (for $\alpha_s(Q^2 = 4m_b^2)$=0.18), $\sigma(e^+e^- \to b\bar{b}b\bar{b})$=9.45(2) pb (for $\alpha_s(Q^2 = M_Z^2)$=0.12), respectively. The cross-section of four b-quark production is approximately 5÷8 times smaller than that for c-quarks, that is due to the kinematical suppression in the production of new heavy $(b\bar{b})$-pair in comparison with lighter $(c\bar{c})$-pair.

The numerical values for the ratios

$$R_{cc\bar{c}\bar{c}} = \frac{\sigma(e^+e^- \to cc\bar{c}\bar{c})}{\sigma(e^+e^- \to c\bar{c})} \tag{25}$$

and

$$R_{bb\bar{b}\bar{b}} = \frac{\sigma(e^+e^- \to bb\bar{b}\bar{b})}{\sigma(e^+e^- \to b\bar{b})} \tag{26}$$

are $R_{cc\bar{c}\bar{c}}$=2.4·10^{-2} (for $\alpha_s(Q^2 = 4m_c^2)$=0.22) and $R_{cc\bar{c}\bar{c}}$=0.7·10^{-2} (for $\alpha_s(Q^2 = M_Z^2)$=0.12). Analogously, $R_{bb\bar{b}\bar{b}}$=2.3·10^{-3} (for $\alpha_s(Q^2 = 4m_b^2)$=0.18) and $R_{bb\bar{b}\bar{b}}$=10^{-3} (for $\alpha_s(Q^2 = M_Z^2)$=0.12).

In Figs.2a,3a,4a we present the momentum, invariant mass and angular distributions for $c(\bar{c})$ quarks. Analogous distributions for $b\bar{b}$ quarks are shown in Figs.2b,3b,4b. These distributions allow one to understand the process picture. According to this picture the emitted $c\bar{c}$ (or $b\bar{b}$) pair moves mainly along the direction of $c(\bar{c})$ (or $b(\bar{b})$) quark, which has emitted the maternal gluon.

4. CROSS-SECTION OF THE B_c MESON PRODUCTION

In this section we will consider the production of the S-wave B_c meson states. The diagrams describing the B_c meson production can be obtained from the diagrams in Figs.1a-d by combining two quark lines into one meson line (see Figs.5a-d).

Our calculations are based on the assumptions that binding energy of heavy quarks (b,c) is much smaller than their masses and, consequently, heavy quarks in the B_c bound state are approximately on-mass-shell.

In this case the p_b and p_c 4-momenta of quarks composing the B_c meson are related to the 4-momentum, P, of the B_c meson in the following way

$$p_b = \frac{m_b}{M}P\,, \qquad p_c = \frac{m_c}{M}P\,, \tag{27}$$

where $M = m_b + m_c$ is the B_c meson mass. Such assumption corresponds to the leading order in the heavy quark effective theory [19].

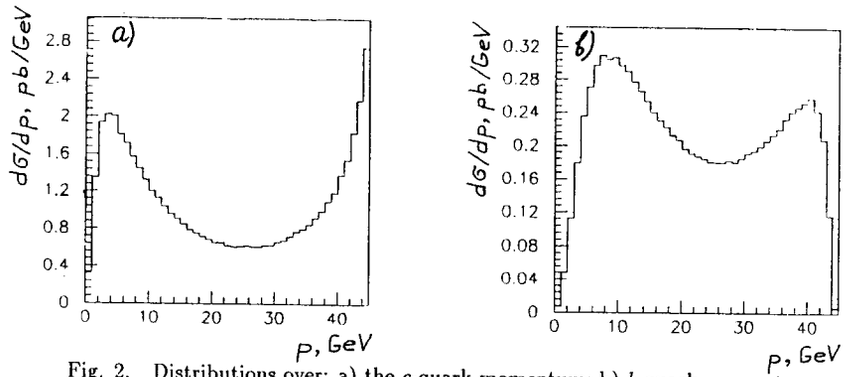

Fig. 2. Distributions over: a) the c-quark momentum; b) b-quark momentum.

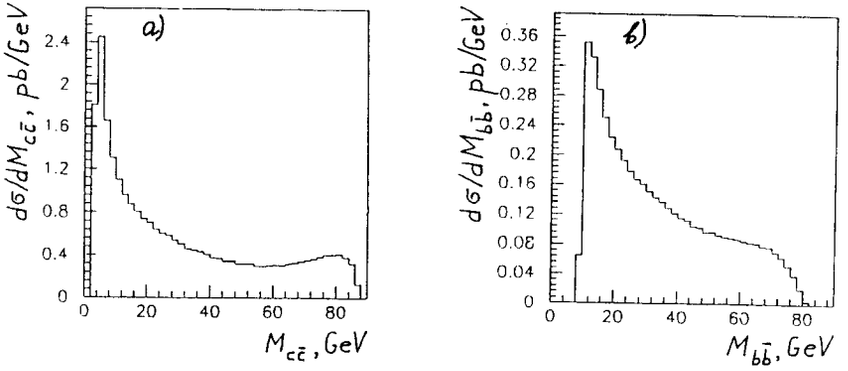

Fig. 3. Distributions over: a) the invariant mass $M_{c\bar{c}} = \sqrt{(p_c + p_{\bar{c}})^2}$; b) the invariant mass $M_{b\bar{b}} = \sqrt{(p_b + p_{\bar{b}})^2}$.

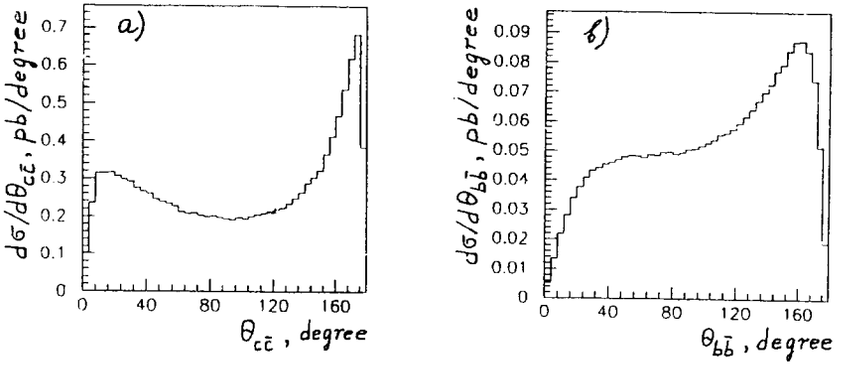

Fig. 4. Distributions over: a) the angle $\theta_{c\bar{c}}$ between c- and $\bar{c}$-quarks momenta; b) the angle $\theta_{b\bar{b}}$ between b- and $\bar{b}$-quark momenta.

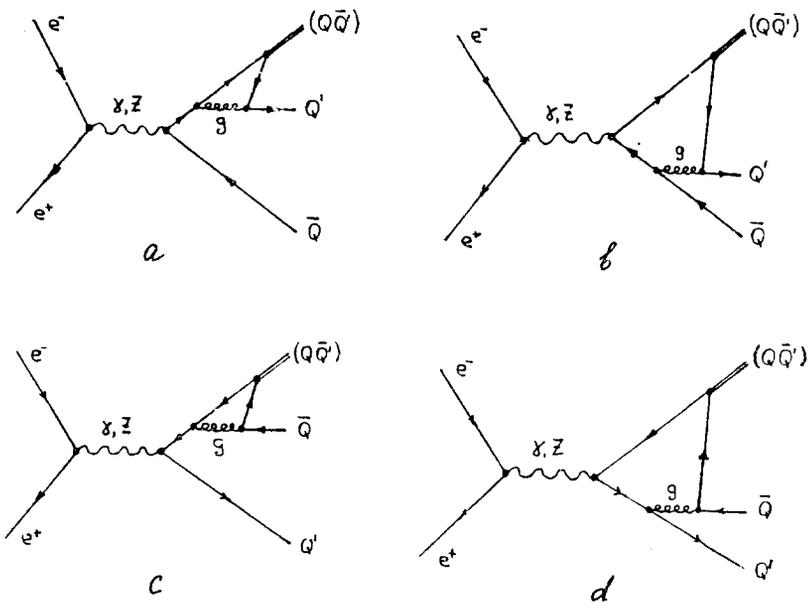

Fig. 5. Feynman diagrams for the $e^+e^- \to (Q\bar{Q}') + Q' + \bar{Q}$ process.

Using the fact that the projection operators

$$\frac{1}{\sqrt{2}}\{v(p,+)\bar{u}(p,+) - v(p,-)\bar{u}(p,-)\} = \frac{1}{\sqrt{2}}(\hat{p} - M)\gamma^5\,, \tag{28}$$

$$\frac{1}{\sqrt{2}}\{v(p,+)\bar{u}(p,+) + v(p,-)\bar{u}(p,-)\} = \frac{1}{\sqrt{2}}(\hat{p} - M)\hat{\varepsilon}^*(p,0)\,, \tag{29}$$

$$v(p,-)\bar{u}(p,+) = \frac{1}{\sqrt{2}}(\hat{p} - M)\hat{\varepsilon}^*(p,+)\,, \tag{30}$$

$$v(p,+)\bar{u}(p,-) = \frac{1}{\sqrt{2}}(\hat{p} - M)\hat{\varepsilon}^*(p,-)\,, \tag{31}$$

where

$$\varepsilon^\mu(p,0) = \frac{E}{M|\vec{p}|}\{\frac{|\vec{p}|^2}{E}, p_x, p_y, p_z\}\,, \tag{32}$$

$$\varepsilon^\mu(p,+) = N\{0, \varepsilon_x, \varepsilon_y, \varepsilon_z\}\,, \tag{33}$$

$$\varepsilon^{\mu}(p,-) = N\{0, -\varepsilon_x^*, -\varepsilon_y^*, -\varepsilon_z^*\} \tag{34}$$

and

$$N = \frac{1}{2\sqrt{2}|\vec{p}|(|\vec{p}|+p_z)}\,, \tag{35}$$

$$\varepsilon_x = -(|\vec{p}|+p_z)^2 + (p_x+ip_y)^2\,, \tag{36}$$

$$\varepsilon_y = -[(|\vec{p}|+p_z)^2 + (p_x+ip_y)^2]i\,, \tag{37}$$

$$\varepsilon_z = 2(|\vec{p}|+p_z)(p_x+ip_y), \tag{38}$$

extract the states with a definite value of total spin, S, and its projection on the z-axis of the system, which is described by the $\bar{u}(p)$ and $v(p)$ spinors ($\varepsilon^{\mu}(p,\lambda)$ is the polarization vector of the vector state with momentum p and helicity λ). Then the amplitude of the $e^+e^- \to B_c\bar{b}c$ process corresponding to the diagrams in Fig.5 can be expressed in terms of these projection operators and helicity amplitudes $M_{h\bar{h}}(\lambda_i)$ calculated in Section 5 in the following way:

$$M(\lambda_i) = \frac{\sqrt{2M}}{\sqrt{2m_b}\sqrt{2m_c}}\Psi(0)\sum_{h,\bar{h}} P_{h,\bar{h}}M_{h,\bar{h}}(\lambda_i)\,, \tag{39}$$

where we imply the summation over helicity states $h, \bar{h}$ of the quark and antiquark composing the B_c-meson. Other fermion helicities are symbolically denoted by λ_i. The projection operators, $P_{h,\bar{h}}$, have the following explicit form ($H = h - \bar{h}$) [20]:

$$P_{h,\bar{h}} = \frac{1}{\sqrt{2}}(-1)^{\bar{h}-1/2}\delta_{H,0} \tag{40}$$

for $^1S_0$-state,

$$P_{h,\bar{h}} = |H| + \frac{1}{\sqrt{2}}\delta_{H,0} \tag{41}$$

for $^3S_1$-state.

The color part of the B_c-meson wave function is $\delta_{ij}/\sqrt{N}$ (N=3). This, being taken into account the color factor F corresponding to the $e^+e^- \to B_c\bar{b}c$ process, is equal to $F = (N^2-1)^2/4N^2$. The wave function value at the origin, $\Psi(0)$, is calculated in the frame of potential model [8], as well as from QCD sum rules [9,11], and it is closely connected with the decay constants, f_{B_c} and $f_{B_c^*}$, of the pseudoscalar (0^-) B_c- and vector (1^-) B_c^*-mesons, respectively, in the following way

$$\Psi(0) = \sqrt{\frac{M}{12}}f_{B_c},$$

where

$$f_{B_c} = f_{B_c^*} = 570 \text{ MeV}.$$

The potentials of different types give practically the same mass values for lowest B_c-meson states. So the pseudoscalar 0^--meson ($1S$-state) mass is fixed by the value of $M = 6.3$ GeV [8]. In this connection, when calculating the B_c-meson bound states of the $1S$-levels we will adopt the values of the b- and c-quarks masses slightly larger than for the case of the free $b\bar{b}c\bar{c}$-quark production, and get them equal to $m_b = 4.8$ GeV and $m_c = 1.5$ GeV. The mass of the $2S$ levels is predicted to be $M = 6.9$ GeV [8]. In this case the b- and c-quark masse values are taken larger — $m_b = 5.1$ GeV and $m_c = 1.8$ GeV. Let us note that the authors of paper [4] do not take into account the effective enhancement of the masses of the b- and c-quarks composing the B_c-meson at the transition to more highly excited states of the B_c-meson. Meanwhile, in the frame of the "on-mass-shell" formalism discussed above it is necessary to do. The wave function value at the origin, $\Psi(0)$, for $2S$-states is $\Psi(0) = 0.275$ GeV$^{3/2}$ [8]. The calculated cross-sections of the B_c- and B_c^*-meson production including the first excited levels are given in Table 2.

Table 2. The cross sections of the B_c (B_c^*)-meson production at $\sqrt{s} = M_Z$, $\alpha_s(Q^2 = 4m_c^2) = 0.22$ and $\alpha_s(Q^2 = M_Z^2) = 0.12$. In the brackets we point out the uncertainty (one standard deviation) in the last figure, which is due to the Monte-Carlo method.

$n^{2S+1}L_J$	1^1S_0	1^3S_1	2^1S_0	2^3S_1
$\sigma(4m_c^2)$, pb	3.105(3)	4.318(3)	0.797(1)	1.064(1)
$\sigma(M_Z^2)$, pb	0.924(1)	1.285(1)	0.2371(3)	0.3168(3)

In accordance with what was said in Section 1 about the cross-section dependence of the $e^+e^- \to b\bar{b}c\bar{c}$ process on the squared value of the transferred momentum, Q^2, in the argument of the $\alpha_s(Q^2)$ function, there arises an uncertainty in the prediction for the B_c-meson production cross-section in the $e^+e^- \to B_c\bar{b}c$ process. In this connection the cross-sections of the $e^+e^- \to B_c\bar{b}c$ process shown in Table 2 and calculated at $Q^2 = s = M_Z^2$ can be considered as pessimistic ones. More optimistic predictions for the number of produced B_c-mesons can be obtained, if we choose the Q^2 value in the $\alpha_s(Q^2)$ argument equal to $Q^2 = 4m_c^2$. The cross-section of the B_c-meson production in this case will be $[\alpha_s(4m_c^2)/\alpha_s(s)]^2 = 3.4$ times large.

It is evident that in these calculations the given value of the total cross-section of the $1S$- and $2S$-state production is equal to 2.76 pb (at $Q^2 = M_Z^2$) is a lower limit. Indeed, the total number of the B_c-meson bound states lying

below the threshold of B- and D-meson production is about 15. All these excited B_c-states due to the cascade radiative decays go over into B_c-meson with the probability equal to 1. So the highest (not only $1S$ and $2S$) excited states should appreciably contribute even due to their large amount. If one takes into account the $\bar{B}_c$-meson production, the cross-section value of the B_c-meson production, obtained above should be doubled.

Let us define the ratio of the $B_c(\bar{B}_c)$-meson number produced (including also the $B_c^*(\bar{B}_c^*)$-states calculated above):

$$R_{B_c} = \frac{\sigma(e^+e^- \to B_c\bar{b}c) + \sigma(e^+e^- \to \bar{B}_c b\bar{c})}{\sigma(e^+e^- \to b\bar{b})}.$$

According to our calculations the R_{B_c} value is $R_{B_c} = 0.6 \cdot 10^{-3}$ at $Q^2 = s$ and $R_{B_c} = 2.0 \cdot 10^{-3}$ at $Q^2 = 4m_c^2$. These R_{B_c} values for the same α_s and $\Psi(0)$ values agree with the calculations performed in recent paper [7]. These values obtained from the QCD perturbation theory expressions one can also compare with the estimate given by the Monte-Carlo program HERWIG, $R_{B_c} = (0.1 \div 1.0) \cdot 10^{-3}$ [18].

Our functions $D(z) = \frac{1}{\sigma}\frac{d\sigma}{dz}$ of the b-quark fragmentation into B_c-meson, where $z = 2|\vec{p}|/\sqrt{s}$ ($|\vec{p}|$ is the B_c-meson momentum), for the case of the pseudoscalar B_c- (curve 1) and vector B_c^*-meson (curve 2) production are shown in Fig.6. The histogram lines correspond to the fragmentation functions calculated by the Monte-Carlo method. The vector mesons fragmentation function (curve 2) when compared with that for the pseudoscalar mesons (curve 1) exhibits a slightly sharper peak in the region around $z = 0.8$ and deep drop at the left side of the peak.

The solid lines in Fig.6 correspond to the fragmentation functions analytically calculated in the limit of $M^2/s \to 0$. One can see that there is a very good agreement between two methods of fragmentation function calculations (see curves 1 and 2). We will present below (in Section 6) detailed calculations of the fragmentation function in this limit and compare our results with those from other papers and, particularly, with the fragmentation function by Peterson et al. [21] marked by 3 in Fig.6.

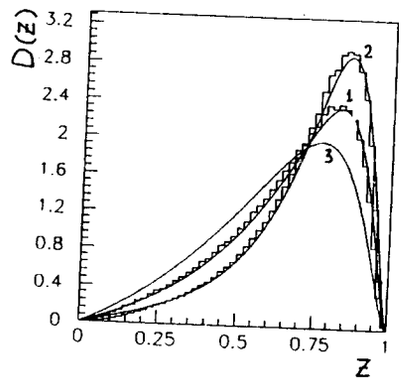

Fig. 6. The fragmentation functions for the pseudoscalar B_c-meson (curve 1) and vector B_c^*-meson (curve 2). The histograms correspond to the Monte-Carlo calculations, but the solid curves correspond to the analytical results. Curve 3 represents the Peterson fragmentation function.

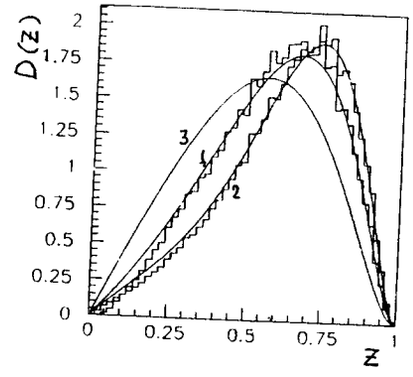

Fig. 7. The fragmentation functions of the pseudoscalar η_c (curve 1) and vector ψ (curve 2) mesons. Other notations are the same as in Fig.6.

Let us note that contrary to the analytical result for the fragmentation functions in [7] our result of the exact Monte-Carlo calculation allows one to obtain the information on the distribution of the particles associated with B_c (for details see [6]).

5. CROSS-SECTIONS OF THE $\eta_c(\psi)$- and $\eta_b(\Upsilon)$-MESON PRODUCTION

The cross-section calculations for these cases are analogous to those for the B_c-meson production case. The only difference lies in other values of the meson masses and wave function $\Psi(0)$ at the origin. The $\Psi(0)$ values are calculated from the quarkonium lepton widths according to the equation

$$\Gamma\left((Q\bar{Q})_{1^-}\right) = 16\pi e_Q^2 \alpha^2 \frac{|\Psi(0)|^2}{M_{Q\bar{Q}}^2}, \qquad (42)$$

where e_Q is the charge of the quarks, which compose the quarkonium, $M_{Q\bar{Q}}$ is the quarkonium mass. Using the well-known experimental values for the quarkonium lepton widths [17] we get for the $c\bar{c}$ bound system the following values of the wave function at the origin: for the $1S$ levels — $\Psi(0) =$

0.208 GeV$^{3/2}$ and for the $2S$ levels — $\Psi(0)$ = 0.156 GeV$^{3/2}$. Different state masses are taken as follows: $m_{c\bar{c}}(1^1S_0)$=2.98 GeV, $m_{c\bar{c}}(1^3S_1)$=3.10 GeV, $m_{c\bar{c}}(2^1S_0)$=$m_{c\bar{c}}(2^3S_1)$=3.69 GeV. The $c(\bar{c})$-quark masses are $m_c = m_{c\bar{c}}/2$, as in (27) we also supposed that $p_c = p_{\bar{c}} = \frac{1}{2}P_{c\bar{c}}$.

The cross-sections of different $c\bar{c}$ bound states at these mass values and wave function values at the origin for two different α_s values are given in Table 3.

Let us define the ratios of the η_c- and ψ-meson numbers including both $1S$- and $2S$-levels to the number of $c\bar{c}$ pairs:

$$R_{\eta_c(\psi)} = \frac{\sigma(e^+e^- \to \eta_c(\psi)c\bar{c})}{\sigma(e^+e^- \to c\bar{c})} . \qquad (43)$$

According to our calculations we have $R_{\eta_c(\psi)}$=3.7·10^{-4} (for $\alpha_s(Q^2 = 4m_c^2)$=0.22) and $R_{\eta_c(\psi)}$=1.1·10^{-4} (for $\alpha_s(Q^2 = M_Z^2)$=0.12).

Table 3. The cross-sections of the $\eta_c(\psi)$-meson production at $\sqrt{s} = M_Z$, $\alpha_s(Q^2 = 4m_c^2) = 0.22$ and $\alpha_s(Q^2 = M_Z^2) = 0.12$. In the brackets we point out the uncertainty (one standard deviation) in the last figure, which is due to the Monte-Carlo method.

$n^{2S+1}L_J$	1^1S_0	1^3S_1	2^1S_0	2^3S_1
$\sigma(4m_c^2)$, pb	1.163(6)	1.069(6)	0.336(2)	0.350(2)
$\sigma(M_Z^2)$, pb	0.346(2)	0.318(2)	0.1000(5)	0.1042(4)

We have also performed the calculations for the bound $b\bar{b}$-system. In this case there are three S-states below the threshold of the B-meson production.

We have used the following wave function values at the origin: for the $1S$ levels — $\Psi(0)$=0.635 GeV$^{3/2}$, for the $2S$ levels — $\Psi(0)$=0.435 GeV$^{3/2}$, and for the $3S$ levels — $\Psi(0)$=0.397 GeV$^{3/2}$. The masses of different $b\bar{b}$ bound states are taken equal to $m_{b\bar{b}}(1^1S_0) = m_{b\bar{b}}(1^3S_1)$ = 9.46 GeV, $m_{b\bar{b}}(2^1S_0) = m_{b\bar{b}}(2^3S_1)$ = 10.02 GeV, $m_{b\bar{b}}(3^1S_0) = m_{b\bar{b}}(3^3S_1)$ = 10.36 GeV. Analogously to the previous case of c-quarks the b-quark mass was taken to be a half of the bound system mass, $m_b = m_{b\bar{b}}/2$. The cross-sections of different $b\bar{b}$-states for two different α_s values are given in Table 4.

Let us define again the ratio of the η_b- and Υ-meson numbers including all the $1S$-, $2S$-, and $3S$-levels to the number of $b\bar{b}$-pairs:

$$R_{\eta_b(\Upsilon)} = \frac{\sigma(e^+e^- \to \eta_b(\Upsilon)b\bar{b})}{\sigma(e^+e^- \to b\bar{b})} . \qquad (44)$$

According to our calculations $R_{\eta_b(\Upsilon)}$=0.9·10^{-4} (for $\alpha_s(Q^2 = 4m_b^2)$=0.18) and $R_{\eta_b(\Upsilon)}$=0.4·10^{-4} (for $\alpha_s(Q^2 = M_Z^2)$=0.12).

Table 4. The cross-section of the $\eta_b(\Upsilon)$-meson production at $\sqrt{s} = M_Z$, $\alpha_s(Q^2 = 4m_b^2) = 0.18$ and $\alpha_s(Q^2 = M_Z^2) = 0.12$. In the brackets we point out the uncertainty (one standard deviation) in the last figure, which is due to the Monte-Carlo method.

$n^{2S+1}L_J$	1^1S_0	1^3S_1	2^1S_0	2^3S_1	3^1S_0	3^3S_1
$\sigma(4m_b^2)$, pb	0.2126(8)	0.2376(8)	0.0810(2)	0.0911(2)	0.0596(2)	0.0675(2)
$\sigma(M_Z^2)$, pb	0.0945(4)	0.1056(4)	0.0360(1)	0.0405(1)	0.0265(1)	0.0300(1)

The form of the c-quark fragmentation into the pseudoscalar η_c- and vector ψ-mesons which is shown in Fig.7 by the curves 1 and 2, respectively, seems to be interesting. The c-quark fragmentation function into the η_c- or ψ-mesons is shifted to the region of small z values as compared to the case of b-quark fragmentation into B_c-meson. The b-quark fragmentation function into η_b- and Υ-mesons are presented in Figs. 8a and 8b, respectively. One can note, that the fragmentation functions of b-quark into $\eta_b(\Upsilon)$-meson and c-quark into $\eta_c(\psi)$-meson are quite similar, though there is an appreciable distinction. This fact will be discussed in detail in the following Section.

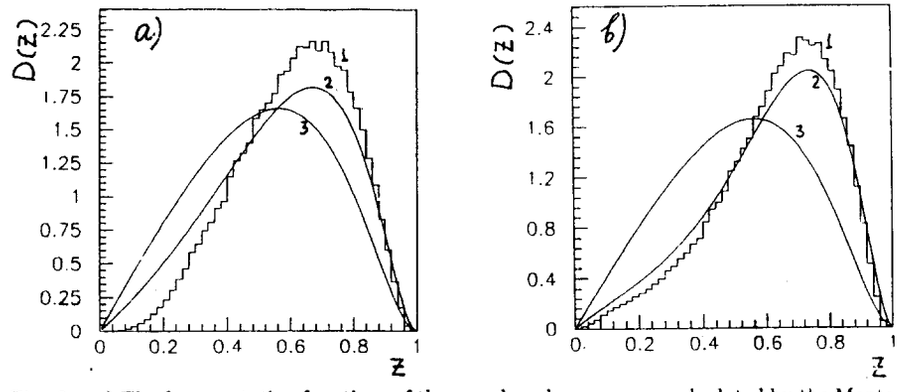

Fig. 8. a) The fragmentation functions of the pseudoscalar η_b-meson calculated by the Monte-Carlo method (curve 1) and analytically (curve 2), curve 3 corresponds to the Peterson fragmentation function; b) the same as in Fig.8a, but for Υ-meson.

In Figs. 9a, 10a, 11a we demonstrate the distributions over invariant masses and angles between $\eta_c(\psi)$-mesons and $c\bar{c}$-quarks, and in Figs. 9b, 10b, 11b we show analogous distributions for $\eta_b(\Upsilon)$-mesons and $b\bar{b}$-quarks. These distributions allow us to state that the processes under discussion have the following characteristic feature. There are two dominating configurations, namely, the first one, when $(Q\bar{Q})$-meson and Q-quark move practically in the same direction opposite to that of residual $\bar{Q}$-quark and the second one, when the $(Q\bar{Q})$-meson and $\bar{Q}$-quark system move in one direction, but Q-quark – in the opposite one.

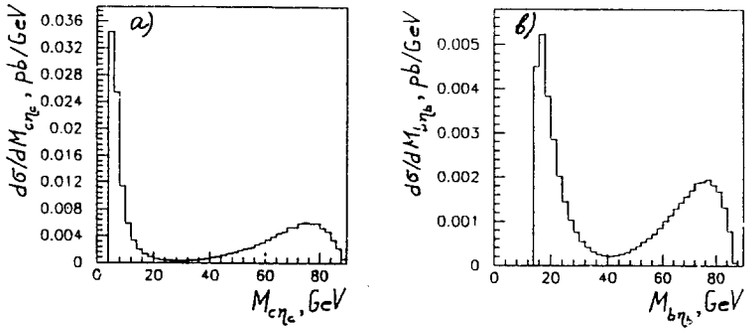

Fig. 9. Distributions over: a) the invariant mass $M_{c\eta_c} = \sqrt{(p_c + p_{\eta_c})^2}$; b) the invariant mass $M_{b\eta_b} = \sqrt{(p_b + p_{\eta_b})^2}$.

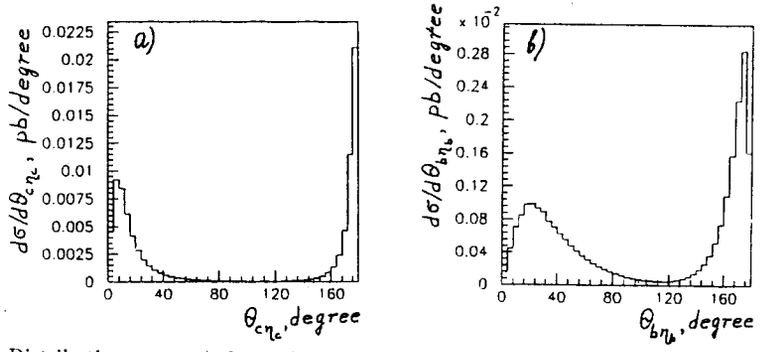

Fig. 10. Distributions over: a) the angle $\theta_{c\bar{\eta}_c}$ between c-quark and η_c-meson momenta; b) the angle $\theta_{b\bar{\eta}_b}$ between b-quark and η_b-meson momenta.

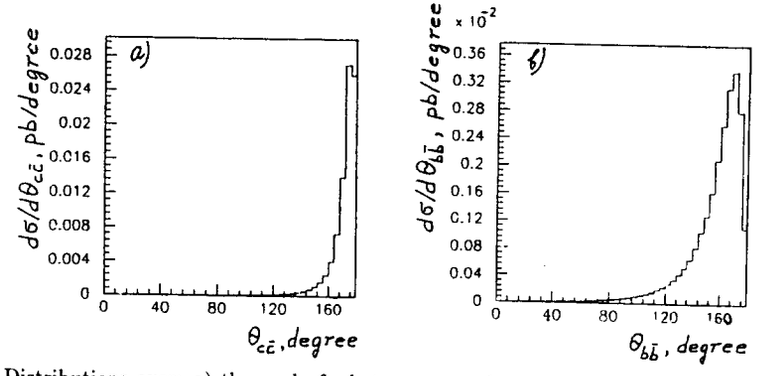

Fig. 11. Distributions over: a) the angle $\theta_{c\bar{c}}$ between c- and $\bar{c}$-quark momenta; b) the angle $\theta_{b\bar{b}}$ between b- and $\bar{b}$-quark momenta.

6. PERTURBATIVE ANALYSIS OF THE HEAVY QUARK FRAGMENTATION FUNCTION

First of all, let us discuss the heavy quark fragmentation into the meson composed of the heavy quarks of different flavours. For concreteness we will consider Z^0-boson decay into b- and c-quarks with their subsequent fragmentation into B_c-meson. The b-quark fragmentation is a dominant one [6]. This process is described by the diagrams analogous to those in Figs.5a,b. The amplitudes corresponding to these diagrams are

$$A_1 = \frac{1}{(X_1)^2}\bar{u}(p_c)\gamma^\mu\Gamma\gamma_\mu(\hat{P} + \hat{p}_c + m_b)\hat{\varepsilon}_Z(v_Z^b - a_Z^b\gamma^5)v(p_{\bar{b}}), \tag{45}$$

$$A_2 = \frac{1}{(1 - rz)X_1}\bar{u}(p_c)\gamma^\mu\Gamma\hat{\varepsilon}_Z(v_Z^b - a_Z^b\gamma^5)(r\hat{P} - \hat{p}_Z + m_b)\gamma_\mu v(p_{\bar{b}}), \tag{46}$$

where $X_1 = y - (1 - z)$, $X_2 = 1 - y$, $z = 2E_{B_c}/M_Z$ and $y = 2E_c/M_Z$ are the fractions of the B_c-meson and c-quark energies, respectively. We denote by r the b-quark and B_c-meson mass ratio — $r = m_b/M$. Other notations are: ε_Z is the Z^0-boson polarization vector, P, p_b, p_c, and p_Z the 4-momenta of the B_c-meson, b-quark, c-quark, and Z^0-boson, respectively, v_Z^b, a_Z^b are the vector and axial couplings of Z^0-boson to b-quarks.

The vertex of the B_c-meson interaction with b- and c-quarks is

$$\Gamma = \gamma_5\frac{(\hat{P} + M)}{2\sqrt{M}}\Psi(0) \tag{47}$$

for the pseudoscalar B_c-meson, and

$$\Gamma = \hat{\varepsilon}\frac{(\hat{P} + M)}{2\sqrt{M}}\Psi(0) \tag{48}$$

for the vector B_c^*-meson.

It is convenient to represent the phase space element in the following form

$$d\Phi = \frac{M_Z^2}{1024\pi^5} dz dy d\cos\theta_{B_c} d\varphi_{B_c} d\varphi_c, \tag{49}$$

where θ_{B_c} and φ_{B_c} are the polar and azimuthal emission angles of B_c-meson (in the rest system of Z^0-boson), φ_c is the c-quark azimuthal angle in the coordinate system, which has the z-axis along the direction of the B_c-meson momentum. As for the cosine of the angle between B_c-meson and c-quark directions, it is expressed through the z and y variables introduced above

$$\cos\theta_c = \frac{zy - 2(z+y) + 2 + 4(1-r)\tau^2}{\sqrt{z^2 - 4\tau^2}\sqrt{y^2 - 4(1-r)^2\tau^2}}, \tag{50}$$

where $\tau = M^2/M_Z^2$. In the Z^0-boson rest system the c-quark momentum is $\vec{p}_c = |\vec{p}_c|\vec{k}$, and the $\vec{k}$ vector components have the following form

$$\begin{aligned} k_x = \sin\theta_c \cos\varphi_c \cos\theta_{B_c} \cos\varphi_{B_c} &- \sin\theta_c \sin\varphi_c \sin\varphi_{B_c} \\ &+ \cos\theta_c \sin\theta_{B_c} \cos\varphi_{B_c}, \end{aligned} \tag{51}$$

$$\begin{aligned} k_y = \sin\theta_c \cos\varphi_c \cos\theta_{B_c} \sin\varphi_{B_c} &+ \sin\theta_c \sin\varphi_c \cos\varphi_{B_c} \\ &+ \cos\theta_c \sin\theta_{B_c} \sin\varphi_{B_c}, \end{aligned} \tag{52}$$

$$k_z = -\sin\theta_c \cos\varphi_c \sin\theta_{B_c} + \cos\theta_c \cos\theta_{B_c}. \tag{53}$$

The integration limits over the y variable (in the leading order in M^2/M_z^2) is

$$y_{min} = (1-z) + \frac{(1-rz)^2}{z(1-z)} \frac{M^2}{M_z^2}, \tag{54}$$

$$y_{max} = 1 - \frac{[1-(1-r)z]^2}{z(1-z)} \frac{M^2}{M_z^2}. \tag{55}$$

The fragmentation function is determined as

$$D(z) = \frac{1}{\Gamma} \frac{d\Gamma}{dz}. \tag{56}$$

The calculations of the amplitudes squared lead to very cumbersome expressions. It is convenient to neglect the small terms of the order of M^2/M_z^2 in the final expressions. Then, the result of the squared amplitude calculations and integration over y, $\cos\theta_{B_c}$, φ_{B_c}, and φ_c variables in the case of the pseudoscalar

B_c-meson production leads to the expression giving the Z^0-boson decay width in the following form:

$$\frac{d\Gamma}{dz} = \frac{2\alpha\alpha_s^2 V |\Psi(0)|^2}{27 M M_z \sin^2\theta_W \cos^2\theta_W (1-r)^2} \frac{M_Z^2}{M^2} \frac{z(1-z)^2}{(1-rz)^6} f_{tot}^{b\to B_c}(z). \tag{57}$$

where $V = (v_Z^b)^2 + (a_Z^b)^2$. The $f_{tot}^{b\to B_c}(z)$ function consists of three parts: $f_{tot}^{b\to B_c}(z) = f_{11}(z) + f_{22}(z) + f_{12}(z)$. The A_1 amplitude squared gives

$$\begin{aligned} f_{11}(z) &= 2 + (2-12r)z + (1 - \frac{14}{3}r + \frac{68}{3}r^2)z^2 \\ &+ (\frac{2}{3}r - \frac{14}{3}r^2 - 12r^3)z^3 + (r^2 + 2r^3 + 2r^4)z^4. \end{aligned} \tag{58}$$

The A_2 amplitude squared leads to

$$f_{22}(z) = 2z^2 - 4rz^3 + 2r^2z^4 \tag{59}$$

and, finally, the term responsible for the A_1 and A_2 amplitude interference gives

$$f_{12}(z) = 4z + (2-16r)z^2 + 16r^2z^3 + (-2r^2 - 4r^3)z^4. \tag{60}$$

The total sum is

$$\begin{aligned} f_{tot}^{b\to B_c}(z) &= 2 + (6-12r)z + (5 - \frac{62}{3}r + \frac{68}{3}r^2)z^2 \\ &+ (-\frac{10}{3}r + \frac{34}{3}r^2 - 12r^3)z^3 + (r^2 - 2r^3 + 2r^4)z^4. \end{aligned} \tag{61}$$

For the case of the vector B_c^*-meson production expression (57) is valid with the substitution of $f_{tot}^{b\to B_c}(z)$ by $f_{tot}^{b\to B_c^*}(z)$. The $f_{tot}^{b\to B_c^*}(z)$ function also consists of three parts. In this case the A_1 amplitude squared gives

$$\begin{aligned} f_{11}(z) &= 2 + (-2-4r)z + (3 - 6r + 12r^2)z^2 \\ &+ (2r - 6r^2 - 4r^3)z^3 + (3r^2 - 2r^3 + 2r^4)z^4. \end{aligned} \tag{62}$$

The A_2 amplitude squared leads to

$$f_{22}(z) = 6z^2 - 12rz^3 + 6r^2z^4 \tag{63}$$

and, finally, the term responsible for the A_1 and A_2 amplitude interference gives

$$f_{12}(z) = (6-12r)z^2 + 12r^2z^3 - 6r^2z^4. \tag{64}$$

The total sum is

$$f_{tot}^{b\to B_c^*}(z) = 2+(-2-4r)z+(15-18r+12r^2)z^2 + (-10r+6r^2-4r^3)z^3+(3r^2-2r^3+2r^4)z^4. \quad (65)$$

Let us note that we have considered the diagrams in Figs.5a,b, where b-quark fragments into $B_c(B_c^*)$-meson. The inclusion of the diagrams in Figs.5c,d leads to the substitutions $r \to (1-r)$ in the resulting expressions, as well as to $v_Z^b \to v_Z^c$ and $a_Z^b \to a_Z^c$. As it is easy to see, the contribution of the diagrams in Figs.5c,d is suppressed with respect to the contribution of the diagrams in Figs.5a,b with ratio of $(m_c/m_b)^2$.

Let us consider now the processes of c-quark fragmentation into $\eta_c(\psi)$-meson. In this case the contributions of all four diagrams in Fig.5 are comparable in magnitude. The amplitudes corresponding to these diagrams have the form

$$A_1 = \frac{1}{(X_1)^2}\bar{u}(p_c)\gamma^\mu\Gamma\gamma_\mu(\hat{P}+\hat{p}_c+\frac{1}{2}M)\hat{\varepsilon}_Z(v_Z^c-a_Z^c\gamma^5)v(p_{\bar{c}}), \quad (66)$$

$$A_2 = \frac{1}{(1-\frac{1}{2}z)X_1}\bar{u}(p_c)\gamma^\mu\Gamma\hat{\varepsilon}_Z(v_Z^c-a_Z^c\gamma^5)(\frac{1}{2}\hat{P}-\hat{p}_Z+\frac{1}{2}M)\gamma_\mu v(p_{\bar{c}}), \quad (67)$$

$$A_3 = \frac{1}{(X_2)^2}\bar{u}(p_c)\hat{\varepsilon}_Z(v_Z^c-a_Z^c\gamma^5)(\hat{p}_c-\hat{p}_Z+\frac{1}{2}M)\gamma^\mu\Gamma\gamma_\mu v(p_{\bar{c}}), \quad (68)$$

$$A_4 = \frac{1}{(1-\frac{1}{2}z)X_2}\bar{u}(p_c)\gamma^\mu(\hat{p}_Z-\frac{1}{2}\hat{P}+\frac{1}{2}M)\hat{\varepsilon}_Z(v_Z^c-a_Z^c\gamma^5)\Gamma\gamma_\mu v(p_{\bar{c}}). \quad (69)$$

The vertexes of the $\eta_c(\psi)$-meson and c-quark interaction are analogous to those of (47) and (48). After the calculations of the matrix element squared and corresponding integrations the result can be represented by expression (57), where one should take $r = 1/2$ and substitute the $f_{tot}^{b\to B_c}(z)$ function by $f_{tot}^{c\to\eta_c(\psi)}(z)$. The $f_{tot}^{c\to\eta_c(\psi)}(z)$ function consists of the following parts

$$f_{tot}^{c\to\eta_c(\psi)}(z) = f_{11}(z)+f_{22}(z)+f_{33}(z)+f_{44}(z)+f_{12}(z) + f_{13}(z)+f_{14}(z)+f_{23}(z)+f_{24}(z)+f_{34}(z). \quad (70)$$

The $f_{13}(z)$, $f_{14}(z)$, $f_{23}(z)$, and $f_{24}(z)$ interference terms vanish in the leading order in M^2/M_z^2, but the remaining terms in the sum are (for the case of the pseudoscalar η_c-meson production)

$$f_{11}(z) = 2-4z+\frac{13}{3}z^2-\frac{7}{3}z^3+\frac{5}{8}z^4, \quad (71)$$

$$f_{22}(z) = 2z^2-2z^3+\frac{1}{2}z^4, \quad (72)$$

$$f_{12}(z) = 4z-6z^2+4z^3-z^4. \quad (73)$$

Other functions are $f_{33}(z) = f_{11}(z)$, $f_{44}(z) = f_{22}(z)$, and $f_{34}(z) = f_{12}(z)$. Finally, for the case of the pseudoscalar η_c-meson production the $f_{tot}^{c\to\eta_c}(z)$ function has the form

$$f_{tot}^{c\to\eta_c}(z) = 4+\frac{2}{3}z^2-\frac{2}{3}z^3+\frac{1}{4}z^4. \quad (74)$$

In the case of the vector ψ-meson production the $f_{13}(z)$, $f_{14}(z)$, $f_{23}(z)$, $f_{24}(z)$ functions are vanishes in the leading order on M^2/M_z^2, but the remaining functions are

$$f_{11}(z) = 2-4z+3z^2-z^3+\frac{5}{8}z^4, \quad (75)$$

$$f_{22}(z) = 6z^2-6z^3+\frac{3}{2}z^4, \quad (76)$$

$$f_{12}(z) = 3z^3-\frac{3}{2}z^4. \quad (77)$$

Other functions are $f_{33}(z) = f_{11}(z)$, $f_{44}(z) = f_{22}(z)$, $f_{34}(z) = f_{12}(z)$. Finally, for the case of the vector ψ-meson production the $f_{tot}^{c\to\psi}(z)$ function has the form

$$f_{tot}^{c\to\psi}(z) = 4-8z+18z^2-8z^3+\frac{5}{4}z^4. \quad (78)$$

As for the $b \to \eta_b(\Upsilon)$ fragmentation functions, they coincide with the $c \to \eta_c(\psi)$ fragmentation functions in the leading order in M^2/M_Z^2. It also should be noted that as the interference terms vanish the fragmentation functions for the symmetric cases of $c \to \eta_c(\psi)$ or $b \to \eta_b(\Upsilon)$ have a simple relationship with the nonsymmetric case of $b \to B_c(B_c^*)$, namely, the fragmentation function for the symmetric case can be obtained from that of the nonsymmetric case through a simple substitution of $r = 1/2$.

In Figs.6 and 7 we show by the solid lines (curves 1 and 2) the results of the analytical calculations performed in the limit of $M^2/M_Z^2 \to 0$ (see expressions (57), (61), (65), (74), (78)), in comparison with the results of the Monte-Carlo method described in Sections 4 and 5. As one can see from these figures, for the case of the b-quark fragmentation into $B_c(B_c^*)$-meson and c-quark into $\eta_c(\psi)$-meson there is a rather good agreement of the analytical and Monte-Carlo results. But in the case of the b-quark fragmentation into $\eta_b(\Upsilon)$-meson (Fig.8) this agreement is only qualitative, which points to a possible significance of the next to the M^2/M_Z^2 terms omitted in this case in the analytical calculations.

It should be noted that there are papers devoted to the calculations of the fragmentation function of a heavy quark into a meson composed of two heavy quarks. In paper [22] the fragmentation function of the heavy quark into the pseudoscalar meson was obtained. In paper [4] the fragmentation function into the vector B_c^*-meson was also calculated. However, the fragmentation functions of b-quark into the pseudoscalar B_c-meson obtained in both [22] and [4] contain mistakes. This problem has already been discussed in our previous paper [6]. Recently papers [7] have been published, where the authors have analytically calculated the fragmentation functions of c-quark into the $\eta_c(\psi)$-meson and b-quark into the $B_c(B_c^*)$-meson in the limit of $M^2/M_Z^2 \to 0$.

The authors of [7] have stressed the fragmentation function universalities and also pointed out their validity in the hadron $p\bar{p}$ collisions. In these papers the calculations have been carried out in the axial gauge taking the $\vec{n}$ vector in a such way that some number of the diagrams vanished in the limit of $M^2/M_Z^2 \to 0$. In the our paper the calculations are performed in covariant gauge and, despite the fact that the contributions of separate diagrams in this case differ from those in [7], the final result summed over all diagrams is the same as in [7]. Let us stress again that in the limit of $M^2/M_Z^2 \to 0$ the fragmentation functions of c-quark into the $\eta_c(\psi)$-meson and b-quark into the $\eta_b(\Upsilon)$-meson coincide. However, our results obtained from the Monte-Carlo method (see Sections 4 and 5) show that in the case of the b-quark fragmentation into the $\eta_b(\Upsilon)$-meson the corrections induced by the terms of the order of M^2/M_Z^2 can be significant.

Let us discuss now the relationship of the analytical expressions obtained in this Section (which are exact in the limit of $M^2/M_Z^2 \to 0$) with the well-known parameterization [21] suggested by Peterson et al. As one can see from equations (57), (61), (65), (74), (78), the asymptotic form of the fragmentation functions is determined by the only parameter, which is the ratio $r = m_Q/M$ of the fragmenting quark mass to meson mass. The fragmentation function behaviour becomes understandable if one considers the z-dependence of the fragmenting quark and gluon propagators. Let Q be the fragmenting quark and Q' is a secondary quark, which couples with Q-quark to produce the $(Q\bar{Q}')$-meson. Neglecting the transverse components we write the 4-momenta, P, of the $(Q\bar{Q}')$-meson and $p_{Q'}$-quark in the following form

$$P = \Big(zp_0 + \frac{M^2}{2zp_0},\ 0,\ 0, zp_0\Big), \tag{79}$$

$$p_{Q'} = \Big((1-z)p_0 + \frac{m_c^2}{2(1-z)p_0},\ 0,\ 0, (1-z)p_0)\Big), \tag{80}$$

where p_0 is the Q-quark momentum modulus. Then, for example, for the diagrams in Fig.5a we have the following expressions for the quark and gluon propagator denominators, $(p_Q^2 - m_Q^2)$ and k^2,

$$p_Q^2 - m_Q^2 \simeq -\Big(m_Q^2 - \frac{M^2}{z} - \frac{m_{Q'}^2}{1-z}\Big) = \frac{M^2(1-rz)^2}{z(1-z)}, \tag{81}$$

$$k^2 = \frac{m_{Q'}}{M}(p_Q^2 - m_Q^2) \simeq \frac{m_{Q'}M(1-rz)^2}{z(1-z)}. \tag{82}$$

The fragmentation function maximum corresponds to the minimal values of the propagator denominators at

$$z_{max} = \frac{M}{M + m_{Q'}}. \tag{83}$$

So, it follows from (81) and (82) that

$$p_Q^2 \simeq (M + m_{Q'})^2, \quad k^2 \simeq 4m_{Q'}^2. \tag{84}$$

For such momentum relation the configuration, when all the Q, $\bar{Q}'$ and Q' quarks move with the same velocity, is realized.

Let us note that expression (81) coincides exactly with the expression used in paper [21] for the calculations of the heavy quark fragmentation amplitude and follows from the inverse proportionality of the amplitude to the energy transferred in the Q-quark decay into $Q\bar{Q}'$-meson and Q'-quark [21]:

$$A \sim \frac{1}{\Delta E} \sim \frac{1}{m_Q^2 - \frac{M^2}{z} - \frac{m_{Q'}^2}{1-z}}. \tag{85}$$

Then

$$D(z) = \frac{N}{z\Big(1 - \frac{\epsilon_1}{z} - \frac{\epsilon}{1-z}\Big)^2}, \tag{86}$$

where N is the normalization factor, and $\epsilon_1 = (1+\sqrt{\epsilon})^2$, $\epsilon = (m_{Q'}/m_Q)^2$. At $\epsilon \ll 1$ equation (86) coincides with the well-known expression for the Peterson parameterization [21]

$$D(z) = \frac{N}{z\Big(1 - \frac{1}{z} - \frac{\epsilon}{1-z}\Big)^2}. \tag{87}$$

Let us note that exact expressions (57,61,65,74,78) can be rewritten in the following form

$$D(z) = \frac{\phi(z,\epsilon)}{z\Big(1 - \frac{\epsilon_1}{z} - \frac{\epsilon}{1-z}\Big)^3}. \tag{88}$$

The Peterson fragmentation function (86) modified for the case of the fragmentation into the heavy quarkonium at the quark mass values used in our exact calculations are shown in Figs.6,7,8 (curves 3). One can see that expression (86) describes the fragmentation function behaviour only in general features, and there is a substantial discrepancy between the exact result and this rough approximations. Expression (86) describes neither the difference in pseudoscalar nor vector meson spectra.

It was shown in [22] that omitting some terms in the explicit expression for the matrix element squared leads to the following expression

$$D(z) = \frac{N' z(1-z)^2(1+(1-r)z)^2}{(1-rz)^4} \sim \frac{\bar{\phi}(z)}{z\left(1-\frac{\epsilon_1}{z}-\frac{\epsilon}{1-z}\right)^2}, \qquad (89)$$

that is close to (86).

It follows from above that the main features of the fragmentation function (maximum location, the behaviour near maximum) are determined by the behaviour of the quark propagators or, which is the same, by the transferred energy value, ΔE. The detailed fragmentation function behaviour depends on the $Q\bar{Q}'$-meson quantum numbers and it is different for pseudoscalar and vector cases(see (57,61,74) and (57,65,78)). In this sense it becomes evident that the fragmentation function parameterization proposed in [21] is a rough approximation for the perturbative calculations of the diagrams in Fig.5.

CONCLUSION

In this paper we have calculated the cross-sections of four heavy quark production in e^+e^--annihilation both for different flavors ,$b\bar{b}c\bar{c}$, and for the same flavors, $c\bar{c}c\bar{c}$, $b\bar{b}b\bar{b}$. In the Z^0-boson pole the cross-section of the $b\bar{b}c\bar{c}$ production is $70 \div 234$ pb and depends on the choice of the value for the transferred momentum squared in the argument of $\alpha_s(Q^2)$. In terms of the $R_{b\bar{b}c\bar{c}}$ ratio, it yields $R_{b\bar{b}c\bar{c}} = (0.8 \div 2.6) \cdot 10^{-2}$ when it is normalized for the $b\bar{b}$-pair production, or $(1.2 \div 3.9) \cdot 10^{-3}$ when it is normalized for the total number of Z^0-bosons (the lowest and upper bounds correspond to two possible choices of the argument in $\alpha_s(Q^2)$). As is expected, the number of Z^0-bosons summed over all experiments at LEP by the fall of 1994, will be $2 \cdot 10^7$, that could correspond to $(2.4 \div 7.8) \cdot 10^4$ of events with the $b\bar{b}c\bar{c}$-quark production.

The calculated values of the $e^+e^- \to c\bar{c}c\bar{c}$ and $e^+e^- \to b\bar{b}b\bar{b}$ process cross-sections bring us to the following ratios of $R_{cc\bar{c}\bar{c}}$ and $R_{bb\bar{b}\bar{b}}$: $R_{cc\bar{c}\bar{c}}$=$2.4 \cdot 10^{-2}$ (for $\alpha_s(Q^2 = 4m_c^2)$=0.22) and $R_{cc\bar{c}\bar{c}}$=$0.7 \cdot 10^{-2}$ (for $\alpha_s(Q^2 = M_Z^2)$=0.12), and,

analogously, $R_{bb\bar{b}\bar{b}}$=$2.3 \cdot 10^{-3}$ (for $\alpha_s(Q^2 = 4m_b^2)$=0.18) and $R_{bb\bar{b}\bar{b}}$=10^{-3} (for $\alpha_s(Q^2 = M_Z^2)$=0.12). Experimental study of these processes can be considered as the way to check the QCD predictions in highest orders of the perturbation theory.

As for the $e^+e^- \to b\bar{b}c\bar{c}$ process, it is also of interest from another point of view. The bound states of the b- and c-quarks (B_c-mesons) predicted by the theory have not yet been discovered. Nevertheless, the discovery and investigation of the B_c-mesons could give important information on quark potential behaviour in the region intermediate with respect to the J/ψ- and Υ-meson families. Assuming that approximate quark-hadron duality does exist, the cross-section of the color singlet $(b\bar{c})$-system production (color factor $F = (N^2-1)^2/4N^2$) in the region of small invariant masses $M_{b\bar{c}}$ can be related to the cross-sections of the B_c-meson bound state production

$$\int_{m_0^2}^{M_{thresh}^2} \frac{d\sigma(e^+e^- \to b\bar{b}c\bar{c})_{(b\bar{c})-sing}}{dM_{b\bar{c}}^2} dM_{b\bar{c}}^2 = \sum \sigma(e^+e^- \to B_c\bar{b}c), \qquad (90)$$

where $m_0 = m_b + m_c \le M_{b\bar{c}} \le M_B + M_D + \Delta M = M_{thresh} (\Delta M \simeq 0.5 \div 1$ GeV). Taking the value of $m_0 = 6.1$ GeV as the boundary value for invariant masses and, for example, $M_{thresh} = 8$ GeV one gets the estimate of the B_c-meson production cross-section equal to $2.07(4) \div 6.9(1)$ pb. This estimate should be compared with B_c-meson cross-section value calculated on the base of the formalism discussed in Section 4.

The cross-section of B_c-meson and its first excitations ($1S$- and $2S$-states), without taking into account other 10 states, whose contributions, according to our expectation, are suppressed in comparison with the case of the $1S$- and $2S$-states, is equal to $2.76 \div 9.3$ pb, which reasonably agrees with the value following from relation (90) assuming the quark-hadron duality.

The fraction of the events with B_c-meson production is $R_{B_c} = (0.6 \div 2.0) \cdot 10^{-3}$ when it is normalized for total $b\bar{b}$-pair production or $(0.9 \div 3.0) \cdot 10^{-4}$, when it is normalized for the total number of Z^0-bosons. For LEP the total number of $2 \cdot 10^7$ of Z^0-bosons is expected. It means that the number of the events with B_c-meson production (including also the events with $\bar{B}_c$-meson production) will be about $(1.8 \div 6.0) \cdot 10^3$. Indeed, the real number of the experimentally reconstructed events will be smaller, because it is also necessary to take into account the branching values of B_c-meson decays into particular modes. Contrary to J/ψ- and Υ-mesons B_c-mesons do not have annihilation type decays into two and three gluons (or photons) and decay through weak channels. From the point of view of experimental identification of the B_c-meson

final state the most promising decay is $B_c \to J/\psi + X$ with the branching value of $\sim 20\%$ and subsequent decay of J/ψ into two muons with the branching value of 6%, which leads finally to $(20 \div 75)$ reconstructed events with $B_c(\bar{B}_c)$-meson production. The B_c-mesons have a large decay length, that can be useful from for the vertex identification of B_c-meson decay. The presence of the vertex detectors as well as the separation of hard leptons in the jets from b- and c-quark decays in the $e^+e^- \to B_c\bar{b}c$ process can also be useful for the final state identification specific to B_c-meson production processes. However, it should be noted that there is large background to this B_c-decay channel, which is due to the decays of charmless B-mesons into J/ψ-mesons. So, the thorough analysis of tl is background is crucial for the identification of B_c-meson events.

Let us note that the cross-section of (bc)-pair production with invariant mass, M_{bc}, in the range of $m_0 \leq M_{bc} \leq M_{thresh}$ (see expression (90)) is also about several pb. It is natural to assume that such pair of bc-quarks capturing a light quark can, with a high probability, fragment into a colorless object, Λ_{bc}-hyperon, which further decays. According to our estimates the amount of such events for $2 \cdot 10^7$ Z^0-bosons should be about several thousands. The observation of a new Λ_{bc}-hyperon, as well as B_c-meson, seems to be an interesting and quite realizable task of the nearest future. Existing now the L3 data on $Br(Z^0 \to J/\psi + X) = 4.1 \cdot 10^{-3}$ are completely explained by the $B \to J/\psi + X$ decays [23] and still not reach in sensitivity the production level due to the fragmentation of $c \to \psi + \bar{c}$.

According to our calculations, the fraction of the events with $\eta_c(\psi)$-meson production (including both the $1S$- and $2S$-levels) is $R_{\eta_c(\psi)}$=3.7·10^{-4} (for $\alpha_s(Q^2 = 4m_c^2)$=0.22) and $R_{\eta_c(\psi)}$=1.1·10^{-4} (for $\alpha_s(Q^2 = M_Z^2)$=0.12), and the fraction with $\eta_b(\Upsilon)$-meson production (taking into account all $1S$-, $2S$-, and $3S$-levels) is $R_{\eta_b(\Upsilon)}$=0.9·10^{-4} (for $\alpha_s(Q^2 = 4m_b^2)$=0.18) and $R_{\eta_b(\Upsilon)}$=0.4·10^{-4} (for $\alpha_s(Q^2 = M_Z^2)$=0.12). It means that at the expected integral LEP luminosity $(2 \cdot 10^7$ Z^0-bosons) the study of such processes will be possible.

In this paper in the frame of the QCD perturbation theory and nonrelativistic heavy quarkonium model we have also performed precise numerical calculations of the fragmentation functions of heavy quarks produced in e^+e^- annihilation at the Z^0-boson pole for the $b \to B_c(B_c^*) + c$, $c \to \eta_c(\psi) + \bar{c}$ and $b \to \eta_b(\Upsilon) + \bar{b}$ processes.

In the scaling limit, where one can neglect small power corrections of the M^2/s type, the analytical expressions for the fragmentation functions of the heavy quark into the vector and pseudoscalar quarkonia have been obtained. These expressions include the symmetric case of the quarkonium with hidden flavor $(Q\bar{Q})$. The resulting single-parameter expression show the difference of

the fragmentation functions into the vector and pseudoscalar quarkonia. We have established a relation of the explicit formulas for the fragmentation functions with Peterson parameterization, that corresponds to the leading terms of the perturbation theory, when the fragmentation function maximum is determined by the behaviour of the fragmenting quark propagator. It is shown that the Peterson parameterization, modified for the case of the parameterization into heavy quarkonium, with physical parameters determined by the heavy quark masses is a rough approximation and differs substantially from the exact fragmentation function.

The authors would like to acknowledge the International Science Foundation (ISF), and one of us (M.V.S.) would like to thank the Russia Foundation of Fundamental Research for financial support.

References

[1] Kiselev V.V., Likhoded A.K., and Tkabladze A.V.//Yad. Phys., 1987. V.46. P.934;
Clavelli L.//Phys. Rev. 1982. V.D26. P.1610.

[2] Kiselev V.V. et al.//Yad. Phys., 1989. V.49. P.1100

[3] Gershtein S.S., Likhoded A.K., Slabospitsky S.R.//Int. J. Mod. Phys. A. 1991. V.13. P.2309.

[4] Chang C.-H., Chen Y.-Q. //Phys Rev. 1992. V.D46. P.3845.

[5] Likhoded A.K, Slabospitsky S.R.//Preprint IHEP 93-23, 1993.

[6] Kiselev V.V., Likhoded A.K., and Shevlyagin M.V. //Yad. Phys., 1994. V.57. P.103.

[7] Braaten E., Cheung K., Yuan T.C.//Preprint NUHEP-TH-93-2, UCD-93-1, 1993; Preprint NUHEP-TH-93-6, UCD-93-9, 1993.

[8] Gershtein S.S. et al., //Yad. Phys., 1988. V.48. P.515.;
Eichten E., Feinberg F.//Phys. Rev. 1981. V.D83. P.2724.;
Godfrey S., Isgur N.//Phys. Rev. 1985. V.D32. P.189.;
Stanley D.P., Robson D.//Phys. Rev. 1980. V.D21. P.3180.;
Kaidalov A.B., Nogteva A.V., //Yad. Phys., 1988. V.47. P.505.;
Kwong W., Romer J.L.//Phys. Rev. 1991. V.D44. P.212.;

Chen Y.-Q., Kuang Y.-P.//Phys. Rev. 1992. V.D46. P.1165.;
Itoh C. et al.//Nuovo Cim. 1992. V.105A. P.1539.

[9] Kiselev V.V., Tkabladze A.V., //Yad. Phys., 1988. V.48. P.536.;
Jibuti G.R., Esakia Sh.,M., //Yad. Phys., 1989. V.50. P.1065.; Yad. Phys., 1990. V.51. P.1681.;
Lusignoli M, Masetti M.//Z. Phys. 1991. V.C51. P.549.

[10] Kiselev V.V., Likhoded A.K., and Tkabladze A.B. //Yad. Phys., 1993. V.56. P.128.;
Kiselev V.V., Tkabladze A.V.//Phys. Rev. 1993. V.D48. P.5208.

[11] Kiselev V.V.//Nucl. Phys. 1993. V.B406. P.340.; Colangelo P., Nardulli G., Paver N.//Z. Phys. 1993. V.C57. P.43.;
Masetti M.//Phys. Lett. 1992. V.B286. P.160.;
Jeukins E. et al.//Nucl. Phys. 1993. V.B390. P.463.;
Aliev T.M., Yilmaz O.//Nuovo Cim. 1992. V.105A. P.827.;
Domingues C.A., Schilcher K., Wu Y.L.//Phys. Lett. 1993. V.B298. P.190.;
Narison S.//Preprint CERN-TH. 7042/93, 1993.

[12] Mele B., Nason P.//Nucl.Phys. 1991. V.B361. P.626., Phys.Lett. 1990. V.B P.635.;
Colangelo G., Nason P.//Preprint LNF-92/017 (P), Frascati, 1992.;
Avaliani I.S., Kartvelishvili V.G. //Preprint IHEP 81-79, Serpukhov, 1981.;
Kartvelishvili V.G., Likhoded A.K., Petrov V.A.//Phys. Lett. 1978. V.B78. P.615;
Kartvelishvili V.G., Likhoded A.K., Slabospitsky S.R.//Sov. J. Nucl. Phys. 1983. V.38 P.952.

[13] Gunion J.F., Kunszt Z.//Phys. Lett. 1985. V.159B. P.167.

[14] Barger V., Stange A.L., Phillips R.J.N. //Phys. Rev. 1991. V.D44. P.1987.

[15] Argyres E.N., Papadopoulos C.G., Vlassopulos S.D.P.// Phys. Lett 1990. V.237B. P.581.

[16] Kleiss R., Stirling W.J.//Nucl. Phys. 1985. V.B262. P.235.

[17] M. Aguilar-Benitez et al. *Review of Particle Properties* //Phys. Rev. 1992. V.D45

[18] Lusignolli M., Masetti M., Petrarka S.//Phys. Lett. 1991. V.B266. P.142.

[19] Isgur N., Wise M.B.//Phys. Lett. 1989. V.B232. P.113; 1990. V.B237. P.527.

[20] Barger V. et al.//Phys. Rev. 1987. V.D35. P.3366.

[21] Peterson C., Schlatter D., Schmitt I., Zerwas P.//Phys. Rev. 1983. V.D27. P.105.

[22] Ji C.R., Amiri F.//Phys. Rev. 1987. V.D35. P.3318.; Phys. Lett. 1987. V.B195. P.593.

[23] L3 Collaboration, Adriani O. et al.//Preprint CERN-PRE/92-99, 1992.

Received February 2, 1994

В.В.Киселев и др.
Рождение четырех тяжелых кварков и связанных состояний в процессах $e^+e^- \to Q + \bar{Q}' + Q' + \bar{Q}$ и $e^+e^- \to (Q\bar{Q}') + Q' + \bar{Q}$ в полюсе Z^o-бозона.

Оригинал-макет подготовлен с помощью системы LaTeX.
Редактор А.А.Антипова. Технический редактор Н.В.Орлова.
Корректор Е.Н.Горина.

Подписано к печати 7.02.1994 г. Формат 60 × 90/16.
Офсетная печать. Печ.л. 1,95. Уч.-изд.л. 2,20. Тираж 250. Заказ 1093.
Индекс 3649. Цена 330 руб. ЛР №020498 06.04.1992.

Институт физики высоких энергий, 142284, Протвино Московской обл.